Author's responses to the reviewer 2.
Seismic attenuation in Antarctic firn

Stefano Picotti[1], José M. Carcione[1,2], and Mauro Pavan[3]

[1]National Institute of Oceanography and Applied Geophysics (OGS), Trieste, Italy.
[2]School of Earth Sciences and Engineering, Hohai University, Nanjing, China.
[3]University of Genova, Italy.

Correspondence: Stefano Picotti (spicotti@ogs.it)

1 Introduction

We thank the reviewer for the valuable and constructive comments on our manuscript.

The reviewer's comments are indicated in italics throughout this letter. Also, new and revised paragraphs that have been included in the main manuscript are indicated by their line numbers. Please note that the equation numbers in this letter do not coincide with those in the revised version of the manuscript.

Based on the points raised below, we have made some improvements to the calculation of velocities and quality factors (sections 4.1 and 4.2). Moreover, we added a discussion to explain in detail the importance of this model for studies related to the physical properties of the firn and the characterization of subglacial materials using amplitude variations with offset (AVO) analysis. Furthermore, we have added a few paragraphs to the Introduction and to the Conclusions, to better explain the main purposes of our work and the possible new applications of the described methodology.

1. *The manuscript "Seismic attenuation in Antarctic firn" submitted by Picotti et al. presents a relevant study addressing the attenuation of seismic P- and S-waves in Antarctic firn. In particular, the authors develop a model based on novel combination of the Biot theory with the concept of fluidized snow filling the pore space. The results shown in the manuscript demonstrate the validity of the proposed approach and its importance for investigations of Antarctic subsurface structures and properties using seismic methods. Accordingly, the study is particularly relevant for the readership of this journal, and thus should be considered for publication after a thorough revision of the manuscript.*

   We thank the reviewer for the clear summary of our work.

2. *In the current version, the objective is indirectly obvious as from the current literature only sparse information regarding seismic wave velocity and attenuation in firn is available. The introduction should clearly state the objective of this study.*

We have modified the paragraph at the beginning of the Introduction (see lines 23 to line 43), to better explain that tools for quantifying the depth dependence of attenuation in ice sheets need to be further developed:

"There are many examples in the literature that used diving waves to estimate the firn velocity-depth structure by picking and inverting first-break traveltimes (e.g., Kirchner and Bentley, 1979; King and Jarvis, 2007; Picotti et al., 2015). The ice-fabric characteristics as a function of depth have been obtained by exploiting the P- and S-wave anisotropic velocities inferred from active-seismic surveys conducted in different settings (e.g., Picotti et al., 2015; Blankenship and Bentley, 1987). However, while tomographic methods for estimating seismic velocity in the whole ice column are well established, algorithms for quantifying the depth dependence of attenuation are underdeveloped. In particular, as far as we know, there are no examples of vertical profiling and modeling of the intrinsic seismic attenuation of P- and S-waves in the polar firn, so far.

Intrinsic loss is often quantified using the inverse quality factor $1/Q$, which represents the fraction of wave energy lost to heat in each wave period (e.g., Carcione, 2022; Gurevich and Carcione, 2022). P-wave quality factors (Q_P) in ice have been measured by several authors in various depth ranges, from values as low as 5 in the temperate ice at the surface of mountain glaciers (e.g., Gusmeroli et al., 2010) up to 700 within cold polar ice caps (e.g., Bentley and Kohnen, 1976). This wide range of values indicates a strong dependence of the quality factor on temperature, demonstrated by laboratory experiments (e.g., Kuroiwa, 1964). This dependence was also verified by Peters et al. (2012) from seismic measurements in Greenland, where Q_P decreases with depth due to an increase in temperature. In this case, Q_P was measured within narrow depth ranges, using strong basal and englacial reflections. Furthermore, it is common practice to measure the average Q_P over the entire ice column using primary and multiple reflection spectra (e.g., Holland and Anandakrishnan, 2009; Booth et al., 2012). Regarding the S-wave quality factor (Q_S), Clee et al. (1969) and Carcione et al. (2021) measured Q_S in warm mountain glacier ice, reporting values of about 23 and 12, respectively. To our knowledge, no other measurements of Q_S in glacial ice or firn have been published in the literature."

We added two paragraphs at the end of the Introduction (starting from line 69, ending 87), in order to better explain the main purposes of our paper:

"In the case of the Antarctic firn, the seismic wave attenuation cannot be explained by adopting a simple porous model consisting of a rigid structure of ice and a porous space filled with air. Such a simple ice-air model underestimates the seismic attenuation by orders of magnitude. Therefore, the fluid saturating the pore space in this case is assumed to be fluidized snow, a mixture of snow particles and air (Mellor, 1974; Maeno and Nishimura, 1979; Nishimura, 1996). In this study we demonstrate that the replacement of air with pore-fluidized snow leads to increased attenuation, and to quality

factor values comparable with those obtained from seismic data. To our knowledge, this is the first attempt to use the concept of fluidized snow as a porous fluid in Biot's theory to model the wave attenuation in firn."

"In the discussion, we give a detailed explanation of the importance of this model for studies related to the physical properties of the firn and to the characterization of subglacial media using amplitude variations with offset (AVO) analysis (e.g., Peters et al., 2008, Booth et al., 2012). We describe an alternative procedure for calculating the average Q_P and Q_S of the ice column below the firn, using the reflected waves at the bottom of the glacier and the Q profile of the firn. This procedure can be useful in cases where conventional methods of amplitude preconditioning for AVO analysis are not applicable."

3. *The authors should be more critical about the uncertainty associated with their results especially with respect to the seismic/mechanical properties of the first (shallowest) layer. How does this rather large standard deviation affect the application of the layer-stripping method?*

We have made some improvements to the calculation of velocities and quality factors. As explained in Sections 3.3 and 4.1, the quality factor profiles obtained using the layer stripping method strongly depend on the thickness and seismic properties of the topmost layer. While these properties are well constrained for the Q_P profile, it was difficult to correctly constrain the topmost layer thickness for the Q_S profile. This is because the velocity of the S-wave near the surface was too low. Therefore, we revised the S-wave velocity curve calculated by Picotti et al. (2015), obtaining an improved version. In this new version (Fig.5a), errors of velocity versus depth are represented, for both P and S waves. We have changed the paragraph on lines 245-251:

" The velocity curves shown in Fig. 5a represent an improved version of those originally presented in Picotti et al. (2015). The uncertainties in the velocities are obtained by perturbing the first-break travel times, according to the dominant frequency of each picked wavelets, and then repeating the Herglotz-Wiechert inversion to obtain different velocity distributions as a function of depth. The mean and standard deviation of the obtained distributions are displayed. The maximum velocities of the P and S waves, verified using the first arrivals refracted at distant offsets on the seismograms acquired using the explosive source, are 3864$\pm$30 m/s and 1947$\pm$25 m/s at 60$\pm$5 m of depth, respectively. At short offsets, errors increase due to the steep velocity gradient near the surface."

The new Figure 5a is shown below (Fig. 1). Then, we modified the text in lines 231-234:

"By calculating the maximum penetration depth of the emerging ray at an offset of 6 m, we estimated the thickness of this layer to be about 1.6 m. Furthermore, the estimated dominant frequency and variance of the source are f_S= 496 Hz and σ_S= 146 Hz, respectively."

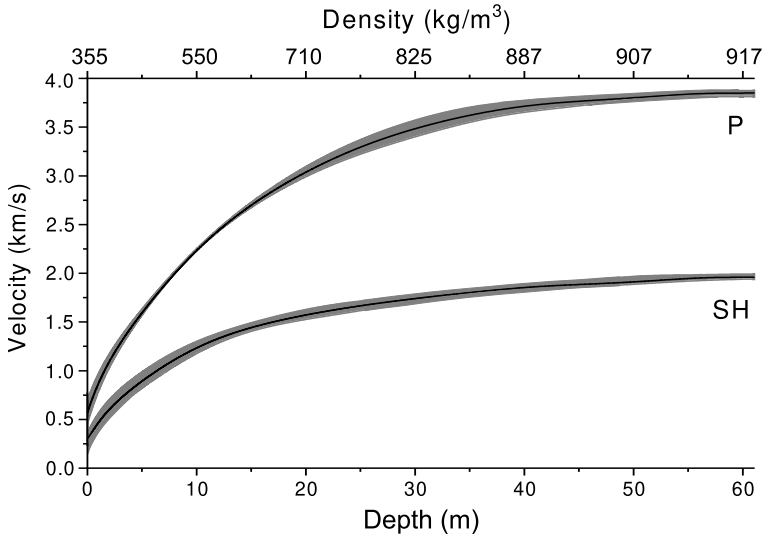

Figure 1. P- and S-wave velocity profiles as a function of depth obtained by using the Hergloz-Wiechert traveltime inversion method, where the error in velocity is represented. The velocity curves are also represented as a function of density using equation (13) proposed by Kohnen (1972).

As expected, after these corrections the shape of the Q_S profile changed, showing lower quality factors in the deeper parts of the firn layer. We modified the text in lines 261-264:

"The second graph (Fig. 10) shows a moderate increase of Q_S, from the previously calculated minimum value of 1.9$\pm$0.4 near the surface, to an average maximum value of about 250$\pm$90, which remains almost constant at depths greater than about 40 m."

Fig. 10 is not attached, but the Q_S plot is displayed in the Figure 2 below. We also modified the text in line 415-417 in the Conclusions:

"The resulting experimental quality factors range from values lower than 5 at the surface to approximately 300 and 250 at about 60 m depth, for P and S waves, respectively."

Regarding the computation of uncertainties, we added two paragraphs at lines 235-240 and 253-258:

"The frequency centroids of the first breaks of the diving P and S waves are obtained from the spectra of the selected waveforms, as described in Picotti and Carcione (2006). The amplitude integrals are calculated, for each wavelet, in a

frequency band from zero to the maximum frequency of the signal. Since this high cut-off frequency depends on the signal-to-noise ratio, a statistic is performed to evaluate the dispersion due to noise. The mean values of the obtained distributions of the frequency centroids, for both the first P and S wave breaks, are shown in Fig. 8. The corresponding standard deviations are less than 3 Hz."

"The two frequency curves shown in Fig. 8, the velocity profiles, the characteristics of the spectral source and Q_P and Q_S of the most superficial layer, are the inputs of the layer-stripping procedure, to calculate the P- and S-wave quality factor profiles of the entire firn column. The uncertainties in Q_P and Q_S profiles are obtained by repeating the procedure using the previously calculated frequency centroid and velocity distributions and perturbing the quality factors of the more superficial layers by their standard deviations. Then, from the two Q-factor distributions in output, we have derived the corresponding profiles of the mean and standard deviation with respect to depth."

In order to improve the theoretical model, we modified the assumptions on the Poisson ratio of the layers. We modified the text in lines 289-306, adding the corresponding new cites:

"The physical properties of the firn layer are obtained from the density model using functions of porosity that have been shown to be suitable for snow. The density profile as a function of depth is obtained by using the following empirical relationship (Kohnen, 1972):

$$\rho(z) = 0.917 \left[1 + \left(\frac{V_{P,ice} - V_P(z)}{2250} \right)^{1.22} \right]^{-1}, \tag{1}$$

where $V_P(z)$ is the vertical P-wave velocity displayed in Fig. 5a, and $V_{P,ice}$ = 3864 m/s is the velocity in ice, which we assume equal to the maximum computed P-wave velocity.

The porosity obtained from the experimental density (1) is

$$\phi(z) = \frac{\rho_s - \rho(z)}{\rho_s - \rho_f}. \tag{2}$$

Fig. 12 shows the experimental density and porosity, where the former increase and the latter decrease monotonically with depth, mainly due to compaction. Then, for each layer, the dry-rock bulk modulus which best fits the data of Johnson (1982) is

$$K_m = K_s(1-\phi)^{30.85/(7.76-\phi)}. \tag{3}$$

The dry-rock shear modulus is

$$\mu = \frac{3}{2}\frac{1-2\nu}{1+\nu}K_m, \quad \nu = 0.38 - 0.36\phi, \tag{4}$$

where ν is the Poisson ratio. For $\phi \leq 9$ % ($\rho \geq 850$ kg/m^3) the medium is mainly ice, and the Poisson ratio is better approximated from the inverted wave velocities as follows

$$\nu = \frac{{V_P}^2 - 2{V_S}^2}{2\left({V_P}^2 - {V_S}^2\right)} \approx 0.32, \tag{5}$$

(Mavko et al., 2009), where V_P and V_S are the P- and S-wave velocities displayed in Fig. 5a, respectively."

Being these assumptions more realistic, the comparison between the experimental and theoretical quality factors also improved, in particular for the S waves (see new Fig. 13, now Fig. 14). The new figure 14 is shown below (Fig.2):

4. *These values were obtained as the average and the standard deviation of the Q factors obtained for traces recorded at 7, 8, 9 and 10 m offset from the source (point)? How does this rather large standard deviation affect the application of the layer-stripping method?*

As explained above, we made some improvements to the computation of velocities and quality factors (and corresponding errors). In the new version (lines 224-225 and 231-232) it is now specified that, together with the average of the quality factors of the shallowest layer, we computed also the standard deviations, both for Q_P and Q_S. In the old version it was indicated an incorrect value of the error for Q_P. In the new version we indicated the correct value: $Q_P = 4.1 \pm 1.3$. The effects of these errors on the application of the layer-stripping method, both for P and S waves, are described in point 3 above.

5. *In the current version, the manuscript does not provide a detailed discussion of the obtained results as reflected by the manuscript structure, which does not include a Discussion section yet solely a section presenting the results.*

A Discussion section has been included (Lines 326-408):

"Studying the structure of polar ice sheets and basal materials is essential for modeling the response of ice masses to climate change. The mechanisms of basal movement of glaciers, which strongly influence the mass balance of Antarctica, are poorly understood. The presence at the ice bottom of enormous quantities of water-saturated sediments, ponds and subglacial lakes, determines the dynamics of the ice streams, which represent the main drainage conduits of ice from the interior of Antarctica to the ocean. Furthermore, the identification and characterization of subglacial lakes is also important for studying the climate history of Antarctica, including the possible presence of extremophile life.

Seismic reflection techniques are powerful tools for mapping the physical properties of subglacial environments, specifically, roughness at the subglacial boundary, water occurrence and fluid layer thickness, rock and sediment type, sediment porosity and fluid saturation, thickness of the subglacial sedimentary layer (e.g., Blankenship et al., 1987). These parameters are all crucial for understanding the basal flow mechanism, which is modulated by the subglacial hydrology

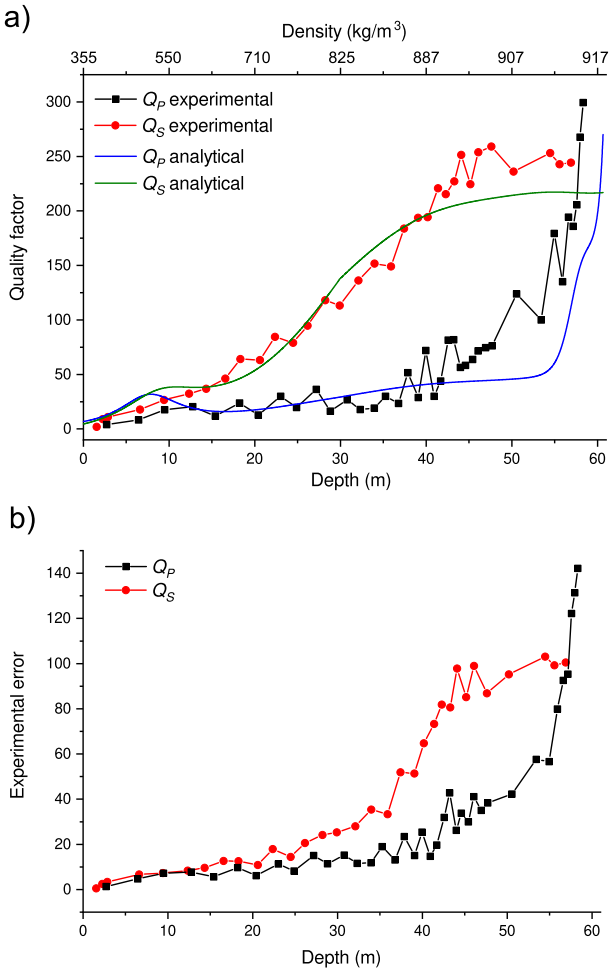

Figure 2. Comparison between the experimental (symbols) and theoretical (solid lines) P- and S-wave quality factors (a) as a function of depth. The quality factors are also represented as a function of density using equation (1) proposed by Kohnen (1972). Experimental errors (b) in the computation of Q_P and Q_S using the layer-stripping frequency-shift method.

and deformation characteristics of the subglacial till. Seismic imaging is the only way to map these properties over large areas, as drilling to the ice bottom is extremely expensive and only provides local information.

The application of advanced AVO techniques has successfully exploited tomographic velocity models and reflection amplitudes at the basal boundary to gather considerable information on the underlying material properties in various contexts (e.g., Blankenship et al., 1987; Anandakrishnan, 2003; Peters et al., 2008; Booth et al., 2012). However, quantitative estimates of these subglacial properties are difficult due to the many challenges that characterize AVO techniques. The two most important limitations are that the source characteristics are often unknown and that the attenuation of P and S waves can be highly variable vertically, across the entire ice column (and in some cases also laterally) and poorly

constrained. Both of these conditions reduce the ability to quantify bedrock reflection coefficients, affecting uncertainties about the physical properties of subglacial materials.

Our method allows for a better understanding of the seismic properties of the firn, which are useful for estimating ice-sheet mass balance from satellite observations of ice-sheet elevation (e.g., Wingham, 2000; Alley et al., 2007). As explained, being Q strongly influenced by the porosity (and density) profile of the propagation medium, measuring both velocities and quality factors has the potential to provide additional information on the physical structure of the firn, avoiding costly coring.

Furthermore, the present work provides alternative means to correct for seismic reflection amplitudes at the glacier floor and can be very useful in cases where conventional amplitude preconditioning methods for AVO analysis are impossible. Indeed, conventional methods ignore the complex Q structure of the firn, and usually rely on the presence of multiple reflections to calculate the source amplitude and average quality factor of the entire ice column at normal incidence (e.g., Holland and Anandakrishnan, 2009; Booth et al., 2012). In addition to the fact that multiple reflections are not always present in seismic data, when available they often show a poor signal-to-noise ratio (e.g., Dow et al., 2013). In the case considered in this work, there is no evidence of multiple reflections in the overall data set. Therefore, the obtained firn velocity-Q profile can help in calculating both the source amplitude and the average quality factor of the ice mass below the firn.

Consider an explosive charge buried deep in the firn (in our case about 27 m for most shots), and a ray propagating from the source to a surface receiver. Adopting our layered firn model, the source amplitude can be calculated considering the first breaks and the equation (7), expressing the decay factor along a distance r_i in each homogeneous layer. Neglecting the transmission loss between adjacent quasi-layers, and indicating with $\alpha_i = \pi/Q_i v_i$ the attenuation factor in the layer i, the total amplitude of the source $S(f)$ is

$$S(f) = GR(f) \prod_{i=1}^{N} \exp\left(\alpha_i f r_i\right) = GR(f) A_c(f), \tag{6}$$

where $A_c(f)$ is the amplitude correction factor, f is the dominant frequency, N is the number of crossed layers, $R(f)$ is the receiver amplitude and G takes into account frequency-independent factors, for example the geometric spreading factor, which is proportional to the total length of the ray. To reduce the uncertainty, the equation (6) can be applied to a large number of receivers for each shot, in order to perform a statistical analysis.

Let us now consider the amplitude $R(f)$ of a signal reflected from the bottom of the glacier. The reflection coefficient R_c is obtained by correcting $R(f)$ for the decay factor as

$$R_c(f) = \frac{GR(f)A_c(f)}{S(f)}, \tag{7}$$

where the calculation of $A_c(f)$ is now performed along the rays reflected from the bed. Therefore, the quality factor profile of the entire ice column is required. In this case, in the absence of englacial reflections, the average quality factor between the firn bottom and the bed is required. This value can be estimated, both for P and S waves, following the

same principle adopted for the calculation of the Q factor in the most superficial layer (direct waves at short offsets) and at the base of the firn (refracted waves at large offsets). This method does not require a priori knowledge of the source characteristics, but only of the firn Q profile. We compare the spectrum of a reference wavelet with those of other wavelets propagating further travel times in both firn and deep ice. For this purpose, we select a reference wavelet at a short offset (ray A) and another wavelet at large offset (ray B), as shown in Fig. 15 (Fig.3 below). These signals travel along raypaths of slight dissimilar length in the firn, while their paths in the underlying ice have very different lengths. The greater the difference between the lengths of these paths, the larger the difference in the centroids of the spectrum and the greater the reliability of the calculated quality factor.

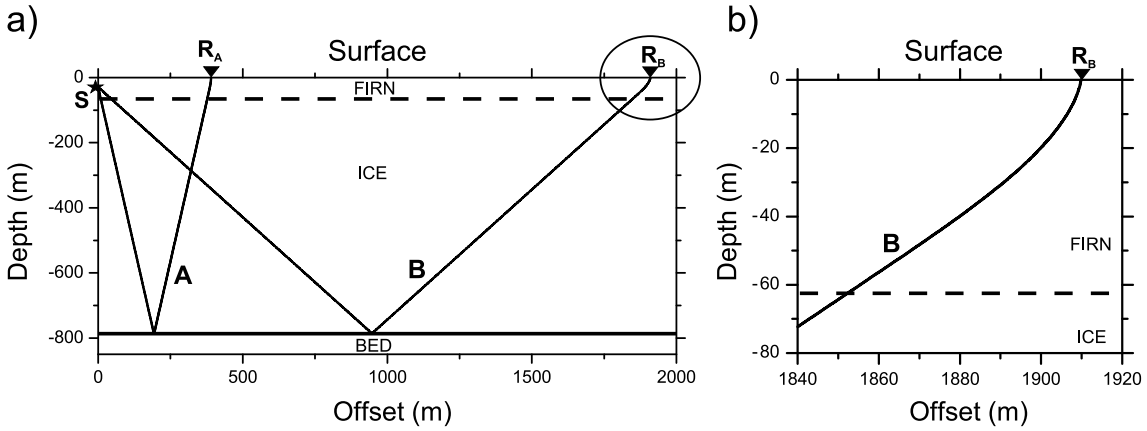

Figure 3. Ray tracing of P waves reflected from bed and emerging at approximately 390 (ray A - reference wavelet) and 1910 m offset (ray B), respectively (a). Magnification of the P-wave ray emerging at the surface (b), in the area highlighted by the circle in Fig. 15a, showing the deflection caused by the velocity gradient in the firn. The source (S), an explosive charge placed at a depth of 27 m, and the receivers (R_A and R_B) are indicated. The surface and ice-bottom interface are almost flat, with slopes less than 1^o

Applying equation (11) to rays B and A we obtain

$$\sum_{rayB} \frac{\Delta t_k}{Q_k} - \sum_{rayA} \frac{\Delta t_k}{Q_k} = \frac{\Delta f_{BA}}{\pi \sigma_A^2}, \tag{8}$$

where Δf_{BA} is the difference between the frequency centroids of the reflected wavelets recorded at the receivers R_B and R_A (Fig. 15). Separating the contributions of ice and firn in the summations, the average quality factor of the ice mass below the firn is

$$Q_{ice} = \frac{\sum_{rayB}^{ice} \Delta t_k - \sum_{rayA}^{ice} \Delta t_k}{\frac{\Delta f_{BA}}{\pi \sigma_A^2} - \left(\sum_{rayB}^{firn} \frac{\Delta t_k}{Q_k} - \sum_{rayA}^{firn} \frac{\Delta t_k}{Q_k} \right)} \tag{9}$$

In the same way we estimated the ice quality factor using the waves refracted at the bottom of the firn, we adopted the dataset acquired with the explosive charges placed at a depth of 27 m (Fig. 3) in order to analyze the reflected waves

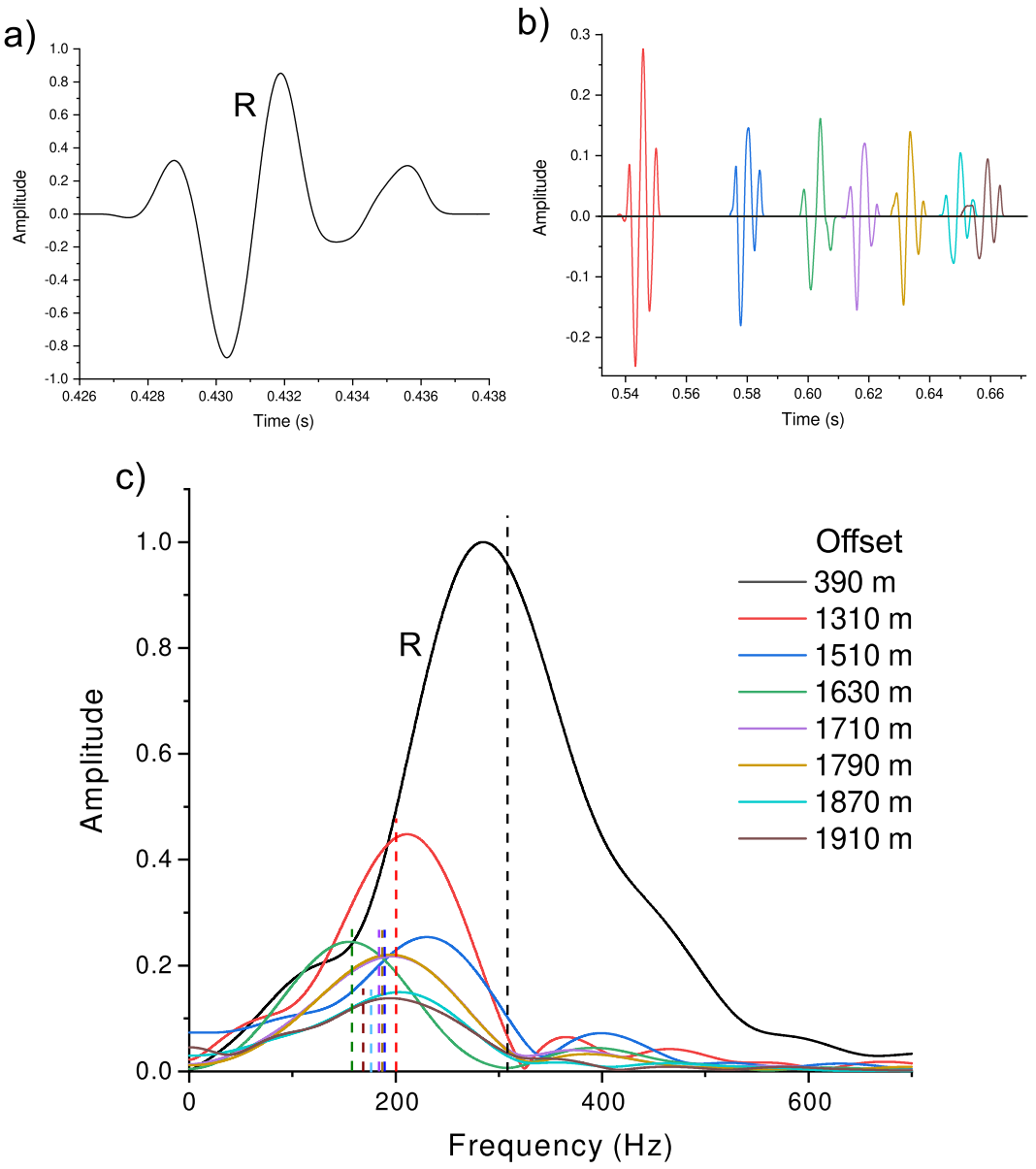

Figure 4. Time histories (b) and corresponding spectra (c) of the P-wave reflected wavelets recorded at long offsets, between 1310 and 1910 m. The label R indicates the reference signal (a) recorded at 390 m offset, while the vertical dashed lines indicate the frequency centroids.

from the glacier bottom. Fig. 16 and Fig. 17 (Fig. 4 and Fig. 5 below) show two examples of selected wavelets and
225 corresponding spectra, up to maximum offset values of 1910 m and 2892 m for P and S waves, respectively. These are the maximum offsets available in our dataset, showing signals with sufficient quality, in terms of signal-to-noise ratio. We performed a ray tracing adopting the algorithm described in Picotti et al. (2015), which allows to calculate the ice

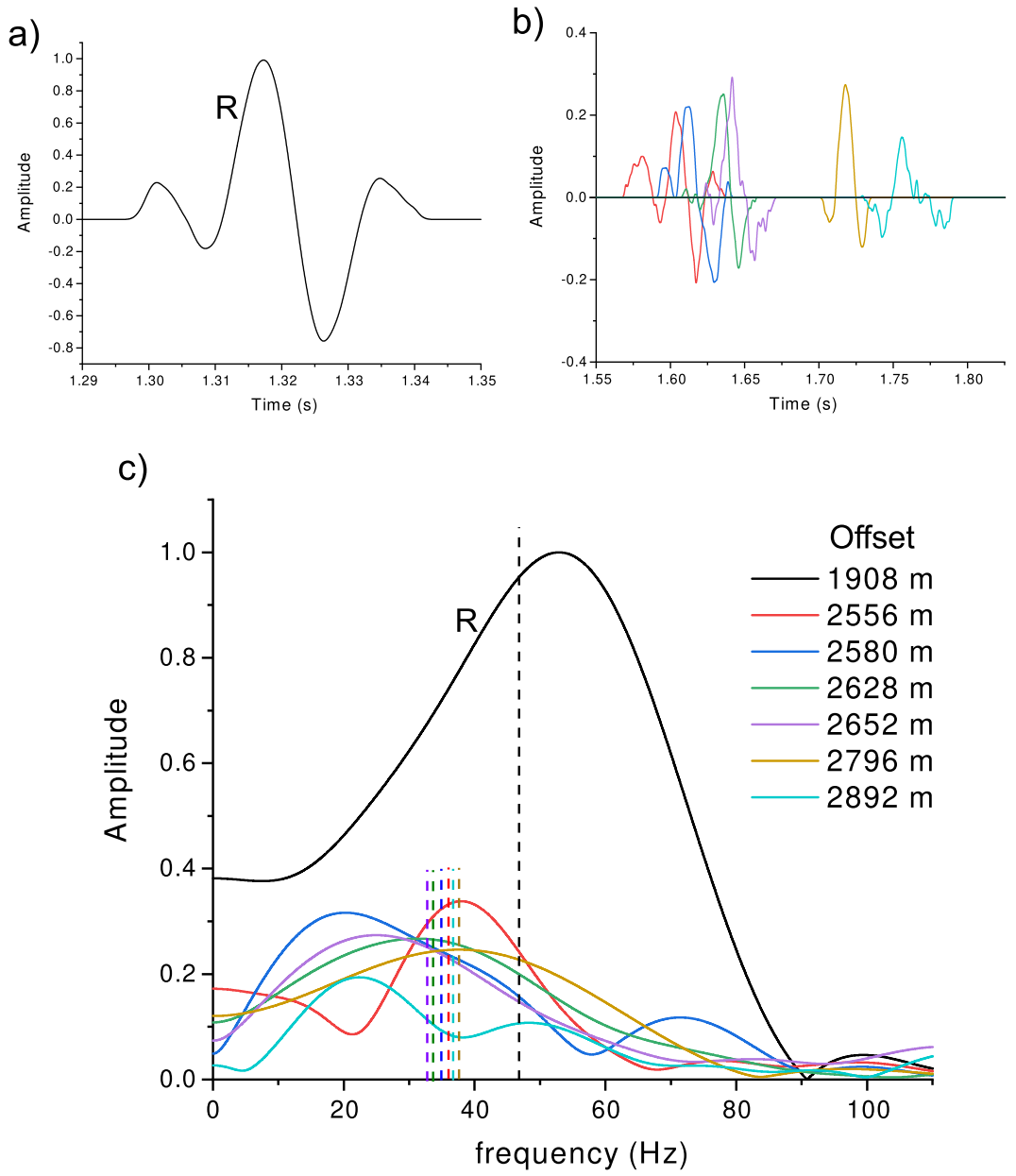

Figure 5. Time histories (b) and corresponding spectra (c) of the S-wave reflected wavelets recorded at long offsets, between 2556 and 2892 m. The label R indicates the reference signal (a) recorded at 1908 m offset, while the vertical dashed lines indicate the frequency centroids.

velocity versus propagation angle. Then, using the wavelet frequency centroids, the firn quality factor profile, and calculated travel times along the ray segments, we obtained the average ice quality factor below the firn using the equation (9).

230 This procedure should be repeated for a large number of selected wavelets, in order to perform a statistical analysis. In

this case, the mean P-wave quality factor of the ice (and standard deviation) is Q_P = 320±70. Using the same procedure, we also analyzed the reflected S waves (Fig. 3b), obtaining an average ice quality factor of Q_S = 205±50. These values agree with the result provided by the diving and refracted waves. However, this analysis shows a slight decrease in ice quality factors, compared to the maximum values estimated at the bottom of the firn. This decrease reflects the substantial dependence of the quality factor on temperature (e.g., Peters et al., 2012; Kuroiwa, 1964), which increases with respect to depth in ice caps and ice streams. In our case, in the SLW site the temperature increases from a minimum value of about -25°C (annual mean temperature) near the surface, to a maximum value at the bed, where the ice temperature is close to its pressure-melting point (Engelhardt and Kamb, 1993; Tulaczyk et al., 2014)."

To support the discussion, new data have been included in the paper. These data are displayed in the new Fig. 3. This plot is shown below (Fig.6) and discussed in the text in lines 110-118:

"All the other data (Fig. 1), aimed at defining the image and anisotropy of the entire ice column, were generated using 0.4 kg PETN (pentaerythritol tetranitrate) charges buried at a depth of 27 m using a hot water drill. Data were recorded on two 48-channel seismic systems and the sensors consisted of alternating single vertical 28 Hz geophones and georods spaced 20 m apart (Fig. 3a). In addition, multi-component data was acquired using three-component continuous recording stations (3C) (Fig. 3b). The 3C stations were first placed along the longitudinal profile, spaced 24 m apart and then moved to the transverse profiles, where the distance was 24 m and 240 m. Each of these stations consisted of a Guralp 40-T broadband seismometer with 40 s corner period, coupled to a Reftek RT-130 data acquisition system equipped with GPS timing. The maximum offset was 4320 m for data recorded using 3C stations and 1910 m for the other data. These data are described in more detail by Horgan et al. (2012) and Picotti et al. (2015)."

6. *The conclusion is a mere summary of the main points of the manuscript, yet it does not interpret the main findings in a broader sense and does not relate them to the objectives stated in the Introduction.*

We added more details to the Conclusions, and two paragraphs in lines 417-421 and 426-430:

"The resulting experimental quality factors range from values lower than 5 at the surface to approximately 300 and 250 at about 60 m depth, for P and S waves, respectively. Thus, the P wave quality factor further increases up to a maximum value of about 380 in the underlying ice. This attenuation model allowed us to infer the average quality factors of the P and S waves of the entire ice column beneath the firn, up to the bed, which is otherwise not possible using standard methods. The estimated average Q factors are slightly lower than the maximum values at the firn bottom, in agreement with the increase in temperature as a function of depth typical of the polar ice caps."

"The knowledge of both the seismic velocity and the attenuation is also important because they could allow, at least theoretically, to obtain the porosity (and density) profile of the polar firn by means of surface or borehole seismic experiments, useful for estimating the ice-sheet mass balance from satellite observations of ice-sheet elevation. In light

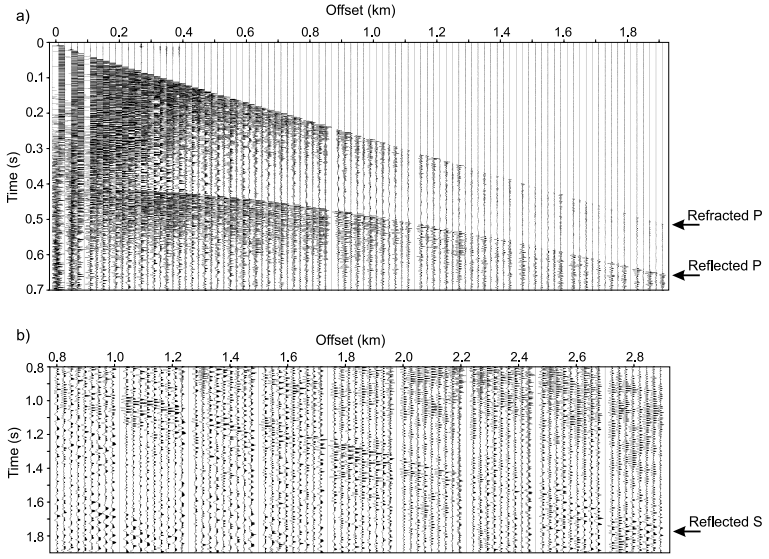

Figure 6. Explosive-charge seismogram recorded by the vertically-oriented geophones and georods along the longitudinal profile (a). Horizontal transverse components showing reflected SH waves from the ice bottom recorded by the 3C stations (b). A 10-400 Hz band-pass filter is applied to remove the surface waves. The wavelets refracted at the bottom of the firn layer and reflected at the ice-sediments interface are indicated.

of this information, surface seismic experiments or well logging in inexpensive hot-water drilled holes could replace costly core drills."

7. *Throughout the manuscript the authors use rather qualitative formulations to describe their results (e.g., "very low/high"). Considering the strong mathematical and physical background of this study such formulations should be avoided by providing a more quantitative interpretation of results or presentation of findings/values reported in the existing literature. Further (more detailed) comments and suggested (technical) corrections can be found in the annotated manuscript file attached here.*

   We accepted most comments and suggested corrections (technical) found in the annotated manuscript. Many qualitative formulations have been eliminated or replaced with quantitative formulations. We would like to point out that many of these expressions were already supported by quantitative explanations.

8. *Lines 235–240: The grains (ice) have the properties K_s = 10 GPa, μ_s = 5 GPa (shear modulus) and ρ_s = 917 kg/m^3 in both layers. The fluid saturating the pores is assumed to be fluidized snow, which is defined as a mixture of snow particles and air, like powder, having zero rigidity modulus. We considerK_f = 571 MPa, ρ_f = 200 kg/m^3 and η = 0.1 Pa s. Reference for these values?*

Lines 250–261: The squirt-flow model has the following values of the parameters: h/R = 0.015, ϕ_c = 0.0002, $K_h = 1.38K_m$, where K_m is the bulk modulus with the grain contacts and cracks open, C = 0.012 kg^2/m^4

Regarding the grain (ice) properties, we cite Gurevich and Carcione (2023) (line 281).
Regarding the squirt-flow model properties, we cite Carcione and Gurevich (2011) (line 310).
Regarding the properties of fluidized snow (K_f, ρ_f and η), there is already a sentence specifying the references in line 283.

We added a paragraph (lines 285–290), and respective references.

"For this study it is important to measure the properties of the fluidized phase of the snow. This task can be performed in coring of firn samples as indicated in Nishimura (1991). The main apparatus consists of two parts: fluidized snow feeder and inclined chute, where it is possible to store the disintegrated snow in fluidized conditions. Measurements are made at a temperature of -15 °C to avoid adhesion effects between snow particles. In this context, bulk density, elastic velocity and viscosity can be measured."

9. *Line 264: "softer layer with much higher porosity". What is "softer" and "much higher", respectively?*

At the beginning of the section we state that "Firn is assumed to be a deposition of two porous media, one snow-like layer with high porosity and the other ice-like with low porosity". Therefore, the term "softer" refers to the layer with higher porosity.

10. *Line 266–267: "strong peak", a strong peak in what? "lower frequencies", quantify.*

We specified "strong relaxation peak (high attenuation)..." (line 317).

11. *Line 280: "amplitude-versus-offset (AVO)". Why was this not mentioned before?*

As indicated in point 2 above, we point out the importance of this study for AVO in a specific paragraph at the end of the introduction. Also, in the new version of the paper we have added a discussion detailing the utility of this model for AVO inversion.